



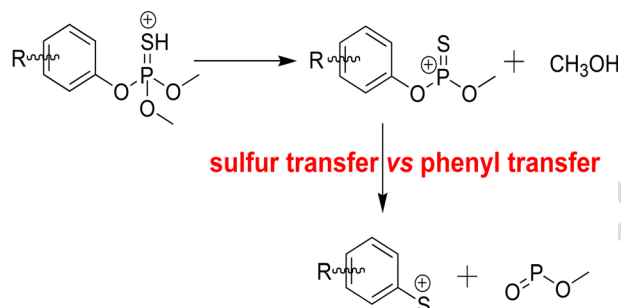
RESEARCH ARTICLE

Sulfur Transfer Versus Phenyl Ring Transfer in the Gas Phase: Sequential Loss of CH₃OH and CH₃O–P=O from Protonated Phosphorothioates

Xiaoping Zhang,¹ Honghan Chen,¹ Yin Ji,¹ Kezhi Jiang,² Huanwen Chen¹

¹Jiangxi Key Laboratory for Mass Spectrometry and Instrumentation, East China University of Technology, Nanchang, 330013, People's Republic of China

²Key Laboratory of Organosilicon Chemistry and Material Technology, Hangzhou Normal University, Hangzhou, 311121, China



Abstract. Collisional activation fragmentation of protonated phosphorothioates leads to skeletal rearrangement and formation of aryl sulfenyl cation (R-PhS⁺) via successive eliminations of CH₃OH and CH₃O–P=O. To better understand this unusual fragmentation reaction, isotope-labeling experiments and density functional theory (DFT) calculations were carried out to investigate two mechanistic pathways. In route 1, a direct intramolecular transfer of the R-phenyl group occurs from the oxygen atom to the sulfur atom on thiophosphoryl to form methoxy *S*-(3-methyl-4-methylsulfanyl-phenyl) phosphonium thiolate (a4), which subsequently dissociates to form the *m/z* 169 cation. In route 2, the sulfur atom of the thiophosphoryl group undergoes two stepwise transfer (1,4-migration to the *ortho*-carbon atom of the phenyl ring followed by 1,2-migration to the *ipso*-carbon atom) to form an intermediate isomer, which undergoes the subsequent dissociation to form the *m/z* 169 cation. DFT calculations suggested that route 2 was more favorable than route 1 from the point view of kinetics.

Keywords: Sulfur transfer, Phenyl ring transfer, Tandem mass spectrometry, Phosphorothioates, Benzenesulfenyl cation

Received: 5 August 2018/Revised: 22 October 2018/Accepted: 24 October 2018

Introduction

The combination of electrospray ionization mass spectrometry (ESI-MS) with collision-induced dissociation (CID) is commonly used to study the properties of gas-phase ions and mechanisms of gas-phase reactions [1–6]. However, the interpretation of CID spectra is not always straightforward due to various rearrangements that occur during fragmentation [7–14]. The reported rearrangements in the gas-phase included benzyl cation transfer, sulfonyl cation transfer, and halogen

transfer, and have been a subject of many mechanistic studies [7–22].

Sulfur transfer reactions have been increasingly used in organic synthesis [23–27]. Among this class of rearrangement reactions, 1,2-sulfur transfer has been widely investigated and extensively used in the synthesis of heterocycles [23, 28, 29] and in carbohydrate chemistry [30, 31]. The most common pathway of 1,2-sulfur transfer proceeds through a key thiiranium intermediate, which can either undergo elimination to give allyl thioethers or substitution to generate formally transposed substitution products [25]. Other types of sulfur transfer, such as 1,3-sulfur transfer [24] and 1,4-sulfur transfer [32], are rarely described. To the best our knowledge, however, no report has been found on the gas-phase intramolecular sulfur transfer reaction, which deserves further investigation.

Phosphorothioates bearing an S=P bond display important chemical and biological properties that afford utility in various

Electronic supplementary material The online version of this article (<https://doi.org/10.1007/s13361-018-2098-4>) contains supplementary material, which is available to authorized users.

Correspondence to: Kezhi Jiang; e-mail: jiankezhi@hznu.edu.cn, Huanwen Chen; e-mail: chw8868@gmail.com

66 fields, including organic synthesis, medicinal chemistry, mo- 116
 67 lecular biology, and agrochemistry [33, 34]. Previous studies 117
 68 mainly focused on the determination and quantification of 118
 69 phosphorothioates, while few studies focused on their gas- 119
 70 phase fragmentation [35–39]. As an example, a thiono-thiolo 120
 71 rearrangement (Newman-Kwart rearrangement), where the 121
 72 S=P–OR group rearranges to the O=P–SR group via R- trans- 122
 73 fer, can occur under electron ionization or tandem MS [36, 37]. 123
 74 A curious R-PhS⁺ type of ion was observed in the fragmenta- 124
 75 tion of protonated fenthion [36, 40, 41], but no detailed mech- 125
 76 anism has been documented to our knowledge. In this work, an 126
 77 intriguing rearrangement reaction to the formation of R-PhS⁺ 127
 78 ion via sulfur transfer has been investigated in the ESI-MS 128
 79 analysis of phosphorothioates. The mechanism of this reaction 129
 80 was examined in detail by a combination of experimental and 130
 81 theoretical calculation approaches. 131

82 Experimental Section 132

83 *Chemicals and Material* 133

84 Methanol HPLC grade was purchased from Sigma-Aldrich (St. 134
 85 Louis, MO, USA). Fenthion, parathion-methyl (compound 2), 135
 86 fenitrothion (compound 3), tolclofos-methyl (compound 4), 136
 87 and chlorpyrifos-methyl (compound 5) were purchased from 137
 88 J&K Scientific Ltd. (Shanghai, China) with a purity >99%. 138

89 *Mass Spectrometry* 139

90 The samples were analyzed on an LTQ-XL advantage IT- 140
 91 MS (Thermo Scientific, San Jose, CA, USA) and an 141
 92 Orbitrap-XL mass spectrometer (Thermo Scientific, San 142
 93 Jose, CA, USA) using a home-made ESI interface in the 143
 94 positive ion mode. Every diluted solution (1 μg mL⁻¹ in 144
 95 methanol) was infused into the source chamber at a flow 145
 96 rate of 3 μL min⁻¹. The optimized ESI source conditions 146
 97 were as follows: the ion-spray voltage, 3 kV; the nebuliz- 147
 98 ing gas (N₂), 25 arbitrary units (a.u.); the capillary temper- 148
 99 ature, 150 °C, the capillary voltage in 80 V; the tube lens 149
 100 in 100 V. Other parameters were automatically optimized 150
 101 by the system. The ion trap pressure of approximately 1 × 151
 102 10⁻⁵ Torr was maintained with a Turbo pump and pure 152
 103 helium (99.99%) was used as the collision gas. The instru- 153
 104 ment was operated at a high resolution up to 100,000. The 154
 105 CID-MS experiments were performed by using an excita- 155
 106 tion AC voltage to the end caps of the ion trap to include 156
 107 collisions of the isolated ions (isolation width at 1 *m/z*) for 157
 108 a period of 30 ms and variable excitation amplitudes. The 158
 109 CID-MS spectra of the protonated molecules were obtained 159
 110 by activation of the precursor ions at the normalized colli- 160
 111 sion energy of 15%~30%. 161

112 *Theoretical Calculations* 162

113 Theoretical calculations were performed using the Gaussian 09 163
 114 program [42]. The geometries of reactants, transition states, 164
 115 intermediates, and products were optimized using the density 165

functional theory (DFT) method at the B3LYP/6-31+G(d,p) 116
 level. All reactants, intermediates, and products were identified 117
 as true minima in energy by the absence of imaginary frequen- 118
 cies. Transition state (TS) structures were obtained through 119
 relaxed PES scans utilizing DFT method at the B3LYP/6- 120
 31+G(d,p) level to generate initial structures for the TSs, in 121
 which a bond length was scanned to find a first-order saddle 122
 point, and subsequently optimizing the corresponding transi- 123
 tion state. Then, the relevant TS structures are searched and 124
 optimized using either TS or QST2 procedures. QST2 uses a 125
 quadratic synchronous transit approach to get closer to the 126
 quadratic region of the TS and then uses a quasi-Newton 127
 algorithm to complete the optimization. All transition states 128
 were confirmed by the presence of a single imaginary vibra- 129
 tional frequency and the reasonable vibrational mode. Intrinsic 130
 reaction coordinate (IRC) calculations at the same level of 131
 theory were performed on each transition state to further con- 132
 firm that the optimized TS structures were actually connected 133
 to the correct reactants and products by a steepest descend path. 134
 Vibrational frequencies of all the key species were calculated at 135
 the same level of theory. Full structural details and energies of 136
 all structures involved are available in the supplementary ma- 137
 terial. The energies discussed here are the sum of electronic and 138
 thermal free energy. 139

140 Result and Discussion 140

141 *Fragmentation Behavior of Protonated Fenthion* 141

142 The gas phase sulfur transfer rearrangement reaction was ex- 142
 143 plored by investigating the MS fragmentation behavior of 143
 144 protonated fenthion derivatives. Fenthion (compound 1) was 144
 145 selected as a model to perform a detailed investigation. The 145
 146 tandem mass spectrum of protonated fenthion (the mass- 146
 147 isolated *m/z* 279) shown in Figure 1 reveals the formation of 147
 148 a dominant fragment ion at *m/z* 247, corresponding to methoxyl 148
 149 *O*-(3-methyl-4-methylsulfanyl-phenyl) phosphonium thioate, 149
 150 a3 (Supplementary Material Scheme S1) via a neutral loss of 150
 151 32 Da (methanol). Three minor fragment ions are observed at 151
 152 *m/z* 231 (b2), *m/z* 169 (a8), and *m/z* 137 (b1), corresponding 152
 153 to the neutral losses of 48 Da, 110 Da, and 142 Da, respectively 153
 154 (Figure 1(a)). The neutral loss of 48 Da likely arises from 154
 155 elimination of methanethiol. The fragment ion at *m/z* 137 is 155
 156 assigned as 3-methyl-4-methylsulfanyl-benzene cation 156
 157 (Scheme S1), which can be attributed to the loss of *O,O'*- 157
 158 dimethyl thiophosphate from the precursor ion at *m/z* 279. 158
 159 The fragment ion at *m/z* 169 is attributed to 3-methyl-4- 159
 160 methylsulfanyl-benzenesulfenylium cation (Scheme S1) or its 160
 161 isomer, resulted from the elimination of C₂H₇O₃P of the pre- 161
 162 cursor ion, which will be discussed in detailed in the following 162
 163 sections. The elemental compositions of these products were 163
 164 confirmed by accurate mass measurements performed on a 164
 165 high-resolution Orbitrap-XL mass spectrometer (Supplementa- 165
 166 ry Material Figure S1 and Table S1). 166

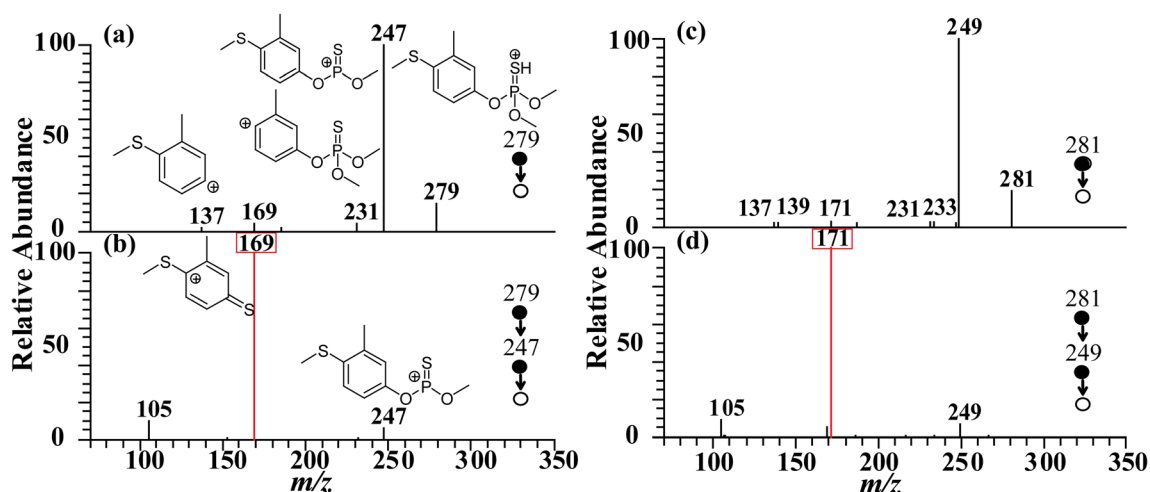


Figure 1. Collision-induced dissociation mass spectra of $[1 + \text{H}]^+$ at the normalized collision energy of 16%. (a) MS^2 spectrum of $[1 + \text{H}]^+$ (m/z 279 \rightarrow), (b) MS^3 spectrum of $[1 + \text{H}]^+$ (m/z 279 \rightarrow m/z 247 \rightarrow), (c) MS^2 spectrum of $[1-^{34}\text{S} + \text{H}]^+$ (m/z 281 \rightarrow), (d) MS^3 spectrum of $[1-^{34}\text{S} + \text{H}]^+$ (m/z 281 \rightarrow m/z 249 \rightarrow)

167 Fragmentation Pathways to *R*-benzenesulfonylium 168 Cation

169 The characteristic fragment ion at m/z 169 can only be
170 interpreted as a result of the $\text{C}_2\text{H}_7\text{O}_3\text{P}$ elimination via sulfur
171 transfer. To interpret the structure of the ion at m/z 169, the MS^3
172 experiments were performed. As shown in Figure 1(b), the
173 MS^3 spectrum of protonated fenthion (m/z 279 \rightarrow m/z 247
174 \rightarrow) shows a base peak ion at m/z 169 via successive elimina-
175 tions of CH_3OH (32 Da) and $\text{CH}_3\text{OP}=\text{O}$ (78 Da). However,
176 there is no relevant moiety of $\text{CH}_3\text{OP}=\text{O}$ in the structure of a3.
177 Thus, the generation of the ion at m/z 169 originated from
178 dissociation of a3 (m/z 247) via skeletal rearrangement.

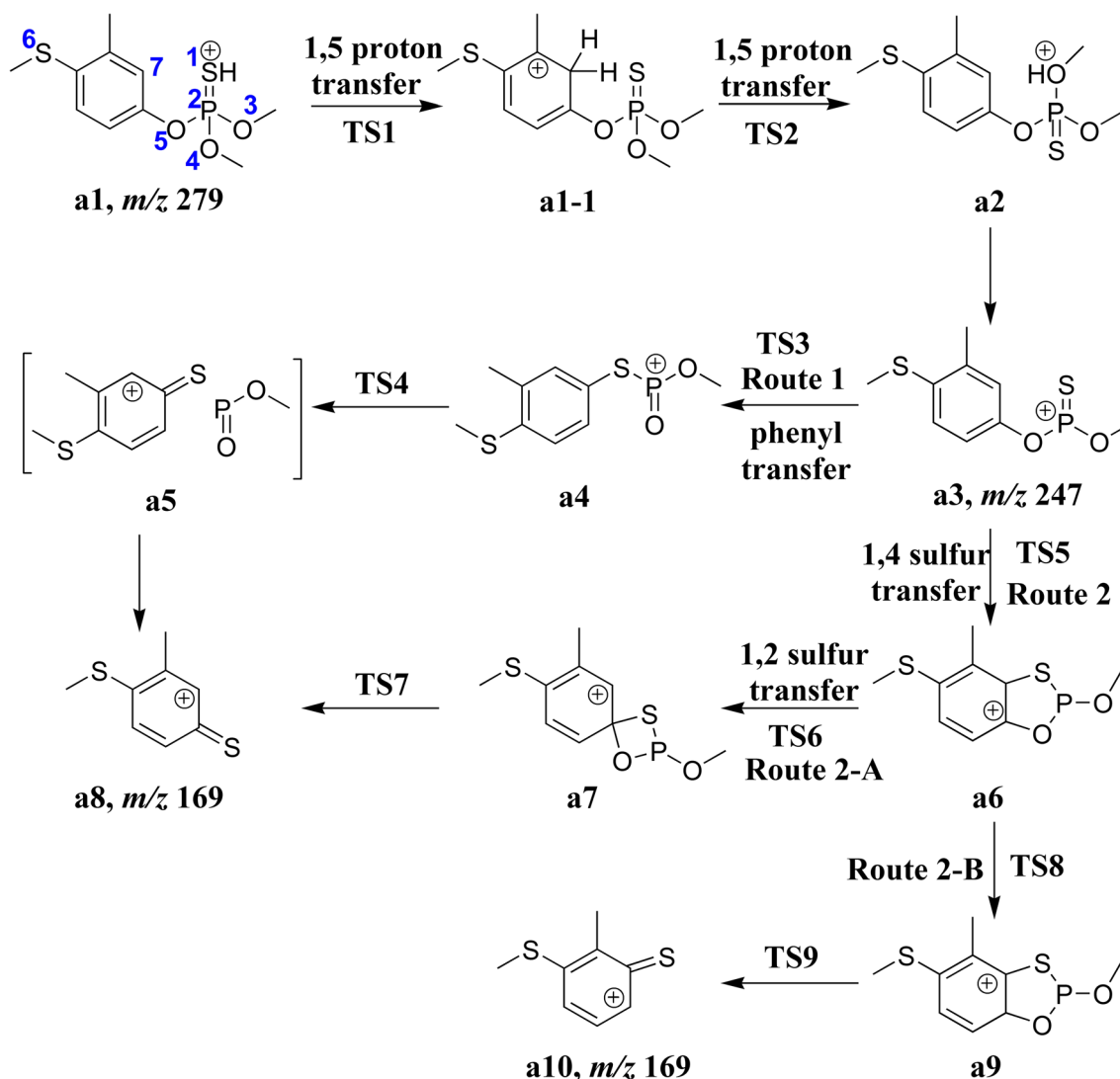
179 Two potential pathways for the generation of m/z 169 from
180 a3 were proposed in Scheme 1. In route 1, a direct transfer of 1-
181 methyl-2-methylsulfanyl-benzene group to *S*1 atom leads to an
182 intermediate a4 (methoxyl *S*-(3-methyl-4-methylsulfanyl-phenyl)
183 phosphonium thiolate), which undergoes the subsequent
184 dissociation to form a8 at m/z 169. An analogous intramolecu-
185 lar *O*- to *S*-benzene migration has also been reported in the gas
186 phase fragmentation diphenyl phosphorochloridothioate using
187 electron impact MS by Cooks [37]. In route 2, the *ortho*-carbon
188 atom of the phenyl ring firstly undergoes a nucleophilic attack
189 on the positively charged $\text{P}=\text{S}$ group, which leads to a bicyclic
190 intermediate a6. Then, the *S*1 atom in a6 undergo a 1,2-migra-
191 tion to form a spiro intermediate a7, which subsequently under-
192 goes the dissociation to give a8 by lose of $\text{CH}_3\text{O}-\text{P}=\text{O}$
193 (route 2-A), or the H atom in *C*7 undergo a 1,2-migration
194 to form a bicyclic intermediate a9, which subsequently undergoes
195 the dissociation to generate a10 by elimination of $\text{CH}_3\text{O}-\text{P}=\text{O}$
196 (route 2-B).

197 The potential pathways in Scheme 1 lead to the product ion
198 at m/z 169 with the structure 3-methyl-4-methylsulfanyl-
199 benzenesulfonylium cation or 2-methyl-3-methylsulfanyl-
200 benzenesulfonylium cation. Benzene-sulfonylium cations have
201 been generated in high abundance by ionization of different
202 precursors containing a thiophenyl group and their gas-phase

203 reactivity has also been reported [14, 43]. Two approaches
204 have been proposed to prepare sulfonylium cations. One is
205 unimolecular sulfur-heteroatom bond fission of “cationoid”
206 complexes or “carriers” of sulfonated compounds, a process
207 usually attempted in the presence of strong Lewis acids [44].
208 The other approach involves the single-electron oxidation of
209 disulfides [45]. The arylthio group (ArS) is of intrinsic interest
210 and has long been incorporated into drug molecules and pep-
211 tides, which can exhibit highly activities such as antiplasmodial
212 activity, and antiviral activity [46–48]. Thus, it is of consider-
213 able interest to investigate the mechanistic formation of the
214 benzenesulfonylium cation (m/z 169).

215 Native ^{34}S Isotope and Isotope Labeling 216 Experiments

217 The postulated decomposition reactions in Scheme 1 were
218 confirmed by the MS/MS analysis on the native ^{34}S isotopic
219 ion (Figure 1(c), (d)) [49]. The sulfur element has two isotopes,
220 ^{32}S and ^{34}S in nature, with the relative abundance at 100% and
221 4.4%, respectively. As shown in Scheme S1, decomposition of
222 the mono isotope ion of a1 (MH^+) at m/z 279 produces the
223 fragment ion b2 at m/z 231 by lose of CH_3SH . The first ^{34}S
224 isotope ion at m/z 281, however, contains two isomeric struc-
225 tures (a1-I1 and a1-I2 in Scheme S2), due to the different
226 position of ^{34}S . As expected, fragmentation of isomer a1-I1
227 gives the product ion b2-I1 at m/z 233, through the neutral loss
228 of $\text{CH}_3^{32}\text{SH}$; whereas dissociation of isomer a1-I2 results in the
229 product ion b2-I2 at m/z 231 via the neutral loss of $\text{CH}_3^{34}\text{SH}$.
230 The almost identical abundance of the two product ions is
231 attributed to the equal distribution of the ^{34}S atom in nature.
232 Interestingly, elimination of $\text{S}=\text{P}(\text{OH})(\text{OCH}_3)_2$ from the iso-
233 topic ion at m/z 281 shows similar fragmentation behavior, with
234 nearly equivalent abundance of the isotopic fragment ions at
235 m/z 137 and m/z 139. The fragment b2-I1 (m/z 137) is gener-
236 ated by the dissociation of isomer a1-I1 through lose of
237 $^{34}\text{S}=\text{P}(\text{OH})(\text{OCH}_3)_2$, while the product ion b2-I2 (m/z 139) is



Scheme 1. Proposed pathways for the generation of the ions at m/z 247 and m/z 169

238 formed via $\text{S}=\text{P}(\text{OH})(\text{OCH}_3)_2$ elimination from a1-I2. The
 239 product ion of a3 m/z 247 (or a8/a10 at m/z 169), however,
 240 has two sulfur atoms in the chemical formula, and thus both
 241 appear as the mono isotopic ion peak with an increasing mass
 242 shift of 2 Da in the CID spectrum. Similarly, as shown in
 243 Figure 1(d), an increasing mass shift of 2 Da was observed
 244 for a8/a10 (from m/z 169 to m/z 171) in the MS^3 spectrum of
 245 protonated ^{34}S isotopologue (m/z 281 \rightarrow m/z 249 \rightarrow).

246 The proposed dissociation pathways in Scheme 1 were also
 247 supported by the CID-MS analysis of the deuterium-labeling
 248 ion (Figure 2). As shown in Scheme 1, there is no external
 249 proton in the product ion a3, and thereby dissociation of $[1 +$
 250 $\text{H}]^+$ and $[1 + \text{D}]^+$ theoretically resulted in a3 with the same
 251 mass (247 Da). However, both the ions at m/z 248 and m/z 247
 252 were observed in the CID mass spectrum of $[1 + \text{D}]^+$, corre-
 253 sponding to the loss of CH_3OH and CH_3OD , respectively. The
 254 existence of the ion at m/z 248 implies that an H/D exchange in
 255 the fragmentation process, e.g. exchange of the external deu-
 256 teron to the *ortho*-positions of phenyl ring via a six-membered
 257 ring. After the deuteron transfers to phenyl ring, the proton or

258 deuterium may migrate back to the methoxyl oxygen competi- 258
 259 tively, which results in subsequent losses of CH_3OH and 259
 260 CH_3OD , respectively. The subsequent transfer of a proton or 260
 261 a deuterium on a1-1 via TS2 for the reaction to proceed was 261
 262 marked by a considerable kinetic isotope effect, $k_{\text{H}}/k_{\text{D}}$. The 262
 263 intensity ratio of elimination of CH_3OH (m/z 248) to elimi- 263
 264 nation of CH_3OD (m/z 247) is about 5:1, which represents the 264
 265 majority of their $k_{\text{H}}/k_{\text{D}}$ value. Our results are consistent with 265
 266 reports of kinetic isotope effect in the range of $k_{\text{H}}/k_{\text{D}} = 5$ during 266
 267 the interannular proton transfer steps of benzylbenzenium ions 267
 268 and 1,4-diphenyl-but-2-yne ions [50]. 268

Density Functional Theory Calculations

269
 270 To further investigate the mechanisms associated with the 270
 271 sulfur and benzene migration reactions, density functional the- 271
 272 ory (DFT) calculations were carried out at the B3LYP/6- 272
 273 31+G(d,p) level of theory. A lone pair of electrons of a hetero- 273
 274 atom is much easier to capture proton [35]. Thus, there are 274
 275 multiple potential protonation sites for fenthion, including S1 275

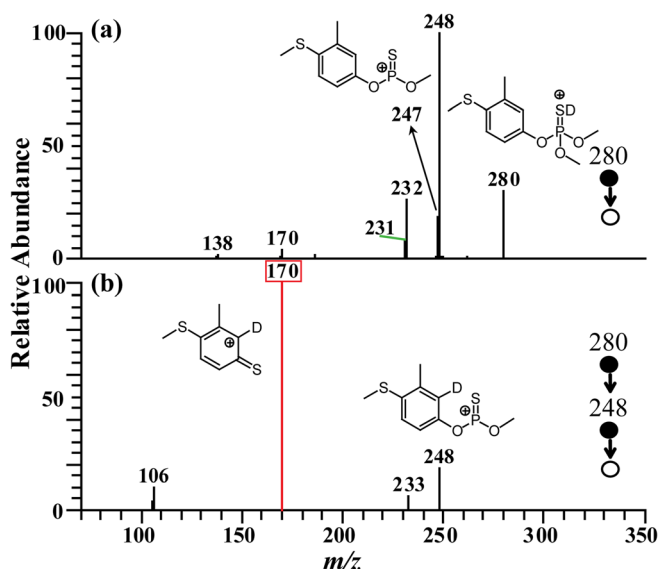


Figure 2. Collision-induced dissociation mass spectra of $[1 + D]^+$. (a) MS^2 spectrum of $[1 + D]^+$ (m/z 280 \rightarrow), (b) MS^3 spectrum of $[1 + D]^+$ (m/z 280 \rightarrow m/z 248 \rightarrow)

276 of the thiophosphoryl, O3/O4 of the methoxy, O5 of the
 277 phenoxy, and S6 of the methyl sulfide (Table 1). The structures
 278 with different protonation sites of fenthion were optimized at
 279 the same level (B3LYP/6-31+G(d,p)) and the relative energies
 280 of these structures are summarized in Table 1. Overall, the
 281 calculation results indicates that S1 atom is the most thermo-
 282 dynamically favorable protonation site, which is 41.3 kJ/mol,
 283 86.4 kJ/mol, 79.7 kJ/mol, and 45.0 kJ/mol lower than proton-
 284 ation site on S6 atom, O3/O4 atom, O5 atom, and C7 atom,
 285 respectively. It has been extensively accepted that the ionizing
 286 proton can transfer to other less favored sites during the sub-
 287 sequent fragmentation process [17, 19].

288 Figure 3 shows a schematic potential energy surface plot for
 289 the generation of a3 (m/z 247). Firstly, the external proton in a1
 290 undergoes a 1,5-migration to the *ortho*-carbon atom of the
 291 phenyl ring via a six-membered ring transition state (TS1) to
 292 afford an isomer a1-1. This process only needs to surmount an
 293 energy barrier of 59.9 kJ mol⁻¹. Then, the activated proton at
 294 the *ortho*-carbon atom of the phenyl ring undergoes 1,5-

295 migration back to the oxygen atom (O3/O4) of the methoxy
 296 group to afford an isomer a2 via a six-membered ring transition
 297 state (TS2), which surmounts an energy barrier of 111.0 kJ mol
 298 ⁻¹. The oxygen atom of the methoxy group in a2 is charged
 299 trivalent oxygen atom. When a2 ion is formed, theoretical
 300 calculations indicates that breakage of the P2–O3/O4 bond
 301 occurs spontaneously, and the two formed fragments are still
 302 held together electrostatically as a stable ion-neutral complex
 303 (INC) [a3/methanol] with a stabilization energy of 49.2 kJ mol
 304 ⁻¹. A direct decomposition of [a3/methanol] results in the
 305 formation of a3.

306 The two potential routes to the ion at m/z 169 in the subse-
 307 quent fragmentations of a3 were compared by theoretical cal-
 308 culations (Figure 4), and details of the corresponding structures
 309 are available in the Supplementary Material. In route 1, the
 310 phenyl ring in a3 is transferred from O5 to S1 through a four-
 311 membered ring transition state (TS3), leading to the formation
 312 of a4 ion with a new carbon-sulfur bond. This process needs to
 313 surmount an energy barrier of 168.3 kJ mol⁻¹. The rearrange-
 314 ment occurs with a concerted process with cleavage of C–O
 315 bond and formation of C–S bond, which can be viewed as an
 316 electrophilic substitution of the phenyl ring (Figure 5). The
 317 conversion of *O*-aryl carbamothioates to *S*-aryl
 318 carbamothioates in the solution-phase is called Newman-
 319 Kwart rearrangement, which is an efficient method for the
 320 straightforward preparation of thiophenol from the correspond-
 321 ing phenols [51]. Migration of phenyl from oxygen to sulfur
 322 has also been observed in spectra of sulphonyl derivatives and
 323 dimethylthiocarbamates in the gas phase [52]. The free energy
 324 of a4 ion is 8.8 kJ mol⁻¹ lower than that of a3 ion. Then, the
 325 formed a4 continues to undergo the cleavage of the P–S bond
 326 induced by the positive charge in P2 atom, and gives rise to an
 327 INC intermediate a5 [3-methyl-4-methylsulfanyl-
 328 benzenesulfonylium cation/metaphosphorous acid methyl ester]
 329 with a small energy barrier of 15.2 kJ mol⁻¹ (TS4). The free
 330 energy of intermediate a5 is 20.2 kJ mol⁻¹ lower than that of a3
 331 ion. The sum free energy of the separated ion a8 and
 332 metaphosphorous acid methyl ester is higher than that of a5
 333 by 46.0 kJ mol⁻¹; this indicates that a5 seems relatively stable
 334 from the view of stabilization energy.

Table 1. Relative energies of $[1 + H]^+$ ions with different protonation sites

| Compound 1 | Site of protonation | Relative energy (kJ mol ⁻¹) |
|------------|---------------------------------|---|
| | S1 of the thiophosphoryl | 0.0 |
| | O3/O4 of the methoxy | 86.4 |
| | O5 of the phenoxy | 79.7 |
| | S6 of the methyl sulfide | 41.3 |
| | C7 of the phenyl ring | 45.0 |

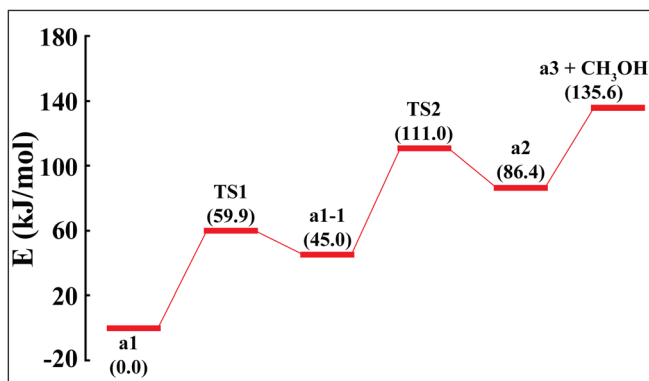


Figure 3. Potential energy diagram for the generation of m/z 247

In route 2, the *ortho*-carbon atom of the phenyl ring firstly undergoes a nucleophilic attack on the positively charged P=S group via a five-membered ring transition state (TS5 in Figure 5), and affords a bicyclic intermediate a6. This process only needs to surmount the energy barrier of 88.1 kJ mol⁻¹. As shown in Figure 5, the length of P-S bond is increased to 2.055 Å in TS5, which appreciably longer than a P=S bond (1.887 Å) and shorter than a covalent P-S bond (2.209 Å). The reason for the elongation of P=S bond in a3 is the formation of five-membered ring by nucleophilic attack of the ring double bond on the positively charged P=S group. The free energy of a6 ion is 18.0 kJ mol⁻¹ lower than that of a3 ion, indicating a more stable structure.

Interestingly, a subsequent 1,2-sulfur transfer in a6 occurs through a three-membered ring transition state (TS6) to afford a7, with a small energy barrier of 59.9 kJ mol⁻¹ (in route 2-A). This sulfur scrambling process is similar to proton scrambling on the phenyl ring [20]. The lengths of two C-S bonds involving sulfur scrambling in TS6 are 2.169 Å and 2.063 Å, respectively. Both are longer than that of a covalent C-S bond (1.738 Å, Figure 5). The four-membered ring structure of a7 seems less stable than the five-membered ring structure of a6. Thus, the ion a7 subsequently undergoes the loss of metaphosphorous acid methyl ester via simultaneous cleavage of the P-S bond and C-O bond (Figure 5). This step is the key step in route 2-A, which surmounts an energy barrier of

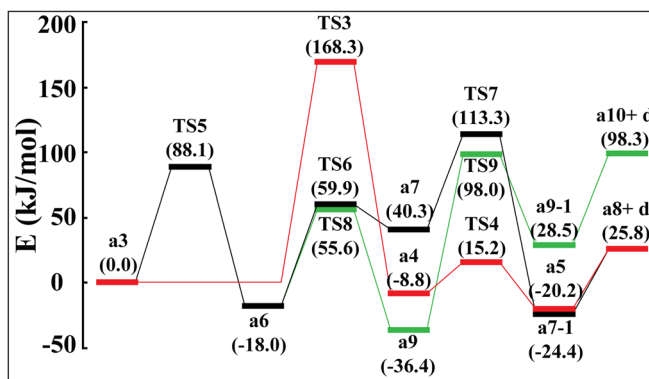


Figure 4. Potential energy diagram for the generation of m/z 169. (red line: route 1, black line: route 2, d: metaphosphorous acid methyl ester)

113.3 kJ mol⁻¹ (TS7). The rearrangement mechanism in route 2-A can be viewed as a successive stepwise of 1,4-sulfur transfer and 1,2-sulfur transfer, then forming a stable 3-methyl-4-methylsulfanyl-benzenesulfonylium cation (a8) via open-ring reaction accompanied by the cleavage of the P-S bond and C-O bond.

Alternatively, a subsequent 1,2-proton transfer in a6 occurs through a three-membered ring transition state (TS8) to afford a9, with a small energy barrier of 55.6 kJ mol⁻¹ (in route 2-B). Then, the ion a9 subsequently undergoes the elimination of metaphosphorous acid methyl ester via direct cleavage of the P-S bond and C-O bond (TS9). This step is the key step in route 2-B, which surmounts an energy barrier of 98.0 kJ mol⁻¹ (TS9). Thus, the rearrangement mechanism of route 2-B can be viewed as a successive stepwise of 1,4-sulfur transfer and 1,2-proton transfer, then forming a stable 2-methyl-3-methylsulfanyl-benzenesulfonylium cation (a10) via opening reaction accompanied by the cleavage of the P-S bond and C-O bond.

The key energy barriers of route 2-A (113.3 kJ mol⁻¹) and route 2-B (98.0 kJ mol⁻¹) are much lower than that of route 1 (phenyl migration, 168.3 kJ mol⁻¹), indicating that sulfur migration is a kinetically more favored process than phenyl migration in the formation of ion at a8 (m/z 169). For route 2-A and route 2-B, the minimum activation energy for the cleavage of the P-S bond and C-O bond process via TS7 and TS9 is 73.0 kJ mol⁻¹ and 134.4 kJ mol⁻¹, respectively, indicating a kinetically more favorable process of route 2-A. Additionally, the sum free energy of the separated ion a8 and metaphosphorous acid methyl ester is 72.5 kJ mol⁻¹ less than that of the separated ion a10 and metaphosphorous acid methyl ester; this indicates that formation of a8 is a thermodynamically favored process. Thus, the formation of a8 in route 2-A is the major path.

The energy requirements for the formation of a8 and metaphosphorous acid methyl ester are 25.8 kJ mol⁻¹ higher than that of a3. However, the free energy of a7-1 is 50.2 kJ mol⁻¹ lower than that of the separated ion a8 and metaphosphorous acid methyl ester; this indicates that a7-1 seems relatively stable from the view of stabilization energy. In addition, the minimum internal excess energy of a7-1 is 137.7 kJ mol⁻¹ or at least 87.5 kJ mol⁻¹ above the separation energy. Thus, direct separation of a7-1 easily occurs in terms of energy, which generates an abundance of ion at m/z 169 (a8).

The Universality of the Gas-Phase Sulfur Transfer

To better delineate the universality of this gas-phase sulfur migration reaction, NO₂-substituted (compounds 2 and 3) and Cl-substituted (compounds 4 and 5) derivatives of fenthion were also investigated by tandem MS experiments, and the tandem MS data (Supplementary Material Figures S2, S3, and S4) were summarized in Table 2. All of these compounds show similar fragmentation behaviors in the MS/MS experiments. Noteworthy, the intensive fragment ions of the corresponding a8 (m/z 154, m/z 168, m/z 191, and m/z 212 for compounds 2, 3, 4, and 5, respectively) were observed for all compounds.

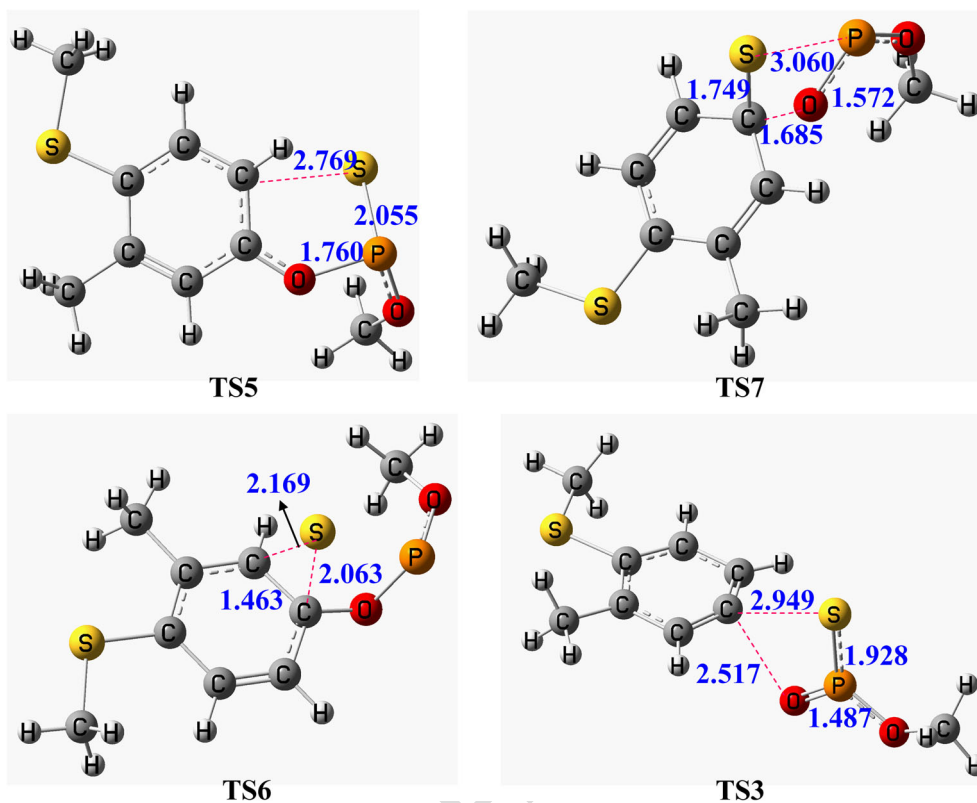
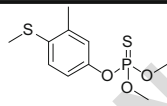
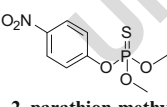
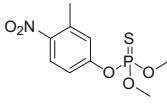
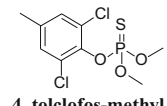
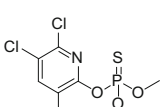


Figure 5. The optimized structures of key intermediates. The bond lengths are given in Å

Table 2. The collision-induced dissociation mass spectra data of $[M + H - \text{CH}_3\text{OH}]^+$ from protonated fenthion derivatives (1–5)

| Compounds | $[M + H]^+$ m/z | $[M + H - \text{CH}_3\text{OH}]^+$ m/z (%) | Loss of 78 Da m/z (%) | Other ions m/z (%) |
|--|----------------------|---|-------------------------------|--|
|  1, fenthion | 279 | 247(5) | 169(100) | 105(10) |
| | 281 | 249(5) | 171(100) | 105(10) |
|  2, parathion-methyl | 264 | 232(10) | 154(3) | 202(100), 200(20), 186(28), 172(7) |
| | 278 | 246(2) | 168(13) | 216(20), 214(10), 200(50), 182(20) |
|  3, fenitrothion | 301 | 269(10) | 191(65) | 254(60), 237(50), 187(80), 175(100) |
| | 303 | 271(25) | 193(70) | 256(60), 239(50), 187(42), 189(43), 177(100) |
|  4, tolclofos-methyl | 305 | 273(60) | 273(85) | 258(72), 241(40), 189(95), 191(53), 179(100) |
| | 322 | 290(2) | 212(100) | 275(25), 230(85), 227(75), 208(77) |
|  5, chlorpyrifos-methyl | 324 | 292(2) | 214(100) | 277(25), 232(95), 229(65), 208(25), 210(40) |
| | 326 | 294(2) | 216(100) | 279(25), 234(97), 231(90), 210(45), 212(25) |

To further investigate the electronic effects of substituents of the sulfur transfer reaction, compounds 2 and 4 were selected as models for comparison of their CID-MS behaviors. The two potential routes (sulfur transfer versus phenyl ring transfer) to the ions at m/z 154 and m/z 191 in the subsequent fragmentations of corresponding ion a3 (m/z 232 and m/z 269) were compared by theoretical calculations (Supplementary Material Figures S5 and S6). According to our calculation results, it could be found that the variation trends of key steps on the potential energy surface diagrams for the generation of m/z 154 and m/z 191 are in accordance with those of m/z 169. As shown in Figures S5 and S6, the key steps in route 1 (phenyl migration) and route 2 (sulfur migration) are TS3 and TS5, respectively. For the formation of ions at m/z 154 and m/z 191, the energy barriers of TS3 and TS5 follows the order: $193.4 \text{ kJ mol}^{-1}$ (TS3 in route 1) $>$ $155.4 \text{ kJ mol}^{-1}$ (TS5 in route 2) and $214.5 \text{ kJ mol}^{-1}$ (TS3 in route 1) $>$ $166.0 \text{ kJ mol}^{-1}$ (TS5 in route 2), respectively, indicating that sulfur migration is a dynamically more favored process in formation of ions at m/z 154 and m/z 191. These experimental and calculation results of fenthion derivatives indicate the universality and the facility of the sulfur transfer reaction in the dissociation process.

Interestingly, for compounds 2 and 3 with a nitro group on the benzene ring, the intensities of the corresponding a8 product declined significantly in the CID-MS, indicating the presence of a nitro group, will inhibit the process of sulfur transfer. Thus, the presence of an NO_2 substituent on the phenyl ring inhibits the sulfur transfer reaction, whereas an $-\text{SCH}_3$ substituent on the phenyl ring promotes this reaction pathway.

Conclusion

In summary, protonated fenthion derivatives firstly dissociates via the elimination of CH_3OH to generate the predominant fragment ion a2 (R-phenoxy, *O*-methyl phosphonium thioate) upon collisional activation. Then, a2 further dissociates via the loss of $\text{CH}_3\text{O}-\text{P}=\text{O}$ to form the arenensulfenylium cations, $\text{R}-\text{PhS}^+$. On the basis of the mass spectra data together with isotope labeling experiments and theoretical calculations, an intriguing mechanism via intramolecular stepwise sulfur transfer has been proposed and validated for this fragmentation reaction. Further research is needed to address the gas-phase reactivity of PhS^+ and related gas-phase ions.

Acknowledgements

This work was supported by the grant from the National Natural Science Foundation of China (Nos. 21520102007, 21605017), Project of Jiangxi Provincial Department of Education (No. GJJ160574), the Research Fund of East China University of Technology (No. DHBK2016131), and the

Jiangxi Key Laboratory for Mass Spectrometry and Instrumentation Open Fund (JXMS201803).

References

- Vukics, V., Guttman, A.: Structural characterization of flavonoid glycosides by multi-stage mass spectrometry. *Mass Spectrom. Rev.* **29**, 1–16 (2010)
- Longevialle, P.: Ion–neutral complexes in the unimolecular reactivity of organic cations in the gas phase. *Mass Spectrom. Rev.* **11**, 157–192 (1992)
- Hopfgartner, G., Bourgoigne, E.: Quantitative high-throughput analysis of drugs in biological matrices by mass spectrometry. *Mass Spectrom. Rev.* **22**, 195–214 (2003)
- Hibbs, J.A., Jariwala, F.B., Weisbecker, C.S., Attygalle, A.B.: Gas-phase fragmentations of anions derived from *N*-phenyl benzenesulfonamides. *J. Am. Soc. Mass Spectrom.* **24**, 1280–1287 (2013)
- Rodriguez, C.F., Cunje, A., Shoeib, T., Chu, I.K., Hopkinson, A.C., Siu, K.W.M.: Proton migration and tautomerism in protonated triglycine. *J. Am. Chem. Soc.* **123**, 3006–3012 (2001)
- Herath, K.B., Weisbecker, C.S., Singh, S.B., Attygalle, A.B.: Circumambulatory movement of negative charge (“ring walk”) during gas-phase dissociation of 2,3,4-trimethoxybenzoate anion. *J. Org. Chem.* **79**, 4378–4389 (2014)
- Zhang, X., Cheng, S.: Intramolecular halogen atom coordinated H transfer via ion–neutral complex in the gas phase dissociation of protonated dichlorvos derivatives. *J. Am. Soc. Mass Spectrom.* **28**, 2246–2254 (2017)
- Zhang, X., Bai, X., Fang, L., Jiang, K., Li, Z.: Decarboxylative coupling reaction in $\text{ESI}(-)\text{-MS/MS}$ of 4-nitrobenzyl 4-hydroxybenzoates: triplet ion–neutral complex-mediated 4-nitrobenzyl transfer. *J. Am. Soc. Mass Spectrom.* **27**, 940–943 (2016)
- Chai, Y., Xiong, X., Yue, L., Jiang, Y., Pan, Y., Fang, X.: Intramolecular halogen transfer via halonium ion intermediates in the gas phase. *J. Am. Soc. Mass Spectrom.* **27**, 1–7 (2016)
- Wang, H.Y., Gao, Y., Zhang, F., Yu, C.T., Xu, C., Guo, Y.L.: Mass spectrometric study of the gas-phase difluorocarbene expulsion of polyfluorophenyl cations via F-atom migration. *J. Am. Soc. Mass Spectrom.* **24**, 1919–1926 (2013)
- Li, F., Zhang, X., Zhang, H., Jiang, K.: Gas-phase fragmentation of the protonated benzyl ester of proline: intramolecular electrophilic substitution versus hydride transfer. *J. Mass Spectrom.* **48**, 423–429 (2013)
- Wang, H.-Y., Xu, C., Zhu, W., Liu, G.-S., Guo, Y.-L.: Gas phase decarbonylation and cyclization reactions of protonated *N*-methyl-*N*-phenylmethacrylamide and its derivatives via an amide Claisen rearrangement. *J. Am. Soc. Mass Spectrom.* **23**, 2149–2157 (2012)
- George, M., Sebastian, V.S., Reddy, P.N., Srinivas, R., Giblin, D., Gross, M.L.: Gas-phase Nazarov cyclization of protonated 2-methoxy and 2-hydroxychalcone: an example of intramolecular proton-transport catalysis. *J. Am. Soc. Mass Spectrom.* **20**, 805–818 (2009)
- Zheng, X., Tao, W.A., Cooks, R.G.: Eberlin reaction of arenensulfenylium cations with cyclic acetals and ketals: ring contraction and cycloreversion. *J. Chem. Soc. Perkin Trans. 2*, 350–355 (2001)
- Wang, S., Dong, C., Yu, L., Guo, C., Jiang, K.: Dissociation of protonated *N*-(3-phenyl-2H-chromen-2-ylidene)- benzenesulfonamide in the gas phase: cyclization via sulfonyl cation transfer. *Rapid Commun. Mass Spectrom.* **30**, 95–100 (2016)
- Wang, S., Yu, L., Wu, Y., Guo, C., Zhang, N., Jiang, K.: Gas-phase fragmentation of protonated *N*,2-diphenyl-*N'*-(*p*-toluenesulfonyl) ethanimidamides: Tosyl cation transfer versus proton transfer. *J. Am. Soc. Mass Spectrom.* **26**, 1428–1431 (2015)
- Sun, H., Chai, Y., Pan, Y.: Dissociative benzyl cation transfer versus proton transfer: loss of benzene from protonated *N*-benzylaniline. *J. Org. Chem.* **77**, 7098–8102 (2012)
- Remeš, M., Roithová, J., Schröder, D., Cope, E.D., Perera, C., Senadheera, S.N., Stensrud, K., Ma, C.-C., Givens, R.S.: Gas-phase fragmentation of deprotonated *p*-hydroxyphenacyl derivatives. *J. Org. Chem.* **76**, 2180–2186 (2011)
- Hu, N., Tu, Y.-P., Jiang, K., Pan, Y.: Intramolecular charge transfer in the gas phase: fragmentation of protonated sulfonamides in mass spectrometry. *J. Org. Chem.* **75**, 4244–4250 (2010)

465
466
467468
469470
471
472
473
474
475
476
477
478
479
480
481
482
483
484
485
486
487
488
489
490
491
492
493
494
495
496
497
498
499
500
501
502
503
504
505
506
507
508
509
510
511
512
513
514
515
516
517
518
519
520
521
522
523
524
525
526
527
528
529
530
531
532
533
534
535

X. Zhang et al.: Sulfur Transfer Versus Phenyl Ring Transfer in the Gas Phase

- 536 20. Hu, N., Tu, Y.-P., Liu, Y., Jiang, K., Pan, Y.: Dissociative protonation and proton transfers: fragmentation of α , β -unsaturated aromatic ketones in mass spectrometry. *J. Org. Chem.* **73**, 3369–3376 (2008) 597
- 537 21. Tu, Y.-P.: Dissociative protonation sites: reactive centers in protonated 598
- 538 molecules leading to fragmentation in mass spectrometry. *J. Org. Chem.* 599
- 540 **71**, 5482–5488 (2006) 600
- 541 22. Hunt, D.F., Giordani, A.B., Shabanowitz, J., Rhodes, G.: Retro-Diels- 601
- 542 Alder, γ -hydrogen rearrangement, and decarboxylation reactions. Path- 602
- 543 ways for fragmentation in the collisions activated dissociation mass 603
- 544 spectra of ketones and carboxylic acid (M–1)⁺ ions. *J. Org. Chem.* **47**, 604
- 545 738–741 (1982) 605
- 546 23. Kim, J.T., Kel'in, A.V., Gevorgyan, V.: 1,2-migration of the thio group in 606
- 547 allenyl sulfides: efficient synthesis of 3-thio-substituted furans and pyr- 607
- 548 roles. *Angew. Chem. Int. Ed.* **115**, 102–105 (2003) 608
- 549 24. Bur, S.K.: 1,3-sulfur shifts: mechanism and synthetic utility. In: 609
- 550 Schaumann, E. (ed.) *Sulfur-Mediated Rearrangements I*, pp. 125–171. 610
- 551 Springer Berlin Heidelberg, Berlin (2007) 611
- 552 25. Sromek, A.W., Gevorgyan, V.: 1,2-Sulfur migrations. In: Schaumann, E. 612
- 553 (ed.) *Sulfur-Mediated Rearrangements I*, pp. 77–124. Springer Berlin 613
- 554 Heidelberg, Berlin (2007) 614
- 555 26. Adam, W., Bargon, R.M.: Synthesis of thiiranes by direct sulfur transfer: 615
- 556 the challenge of developing effective sulfur donors and metal catalysts. 616
- 557 *Chem. Rev.* **104**, 251–262 (2004) 617
- 558 27. Fang, Z., Liu, J., Liu, Q., Bi, X.: [3+2] cycloaddition of propargylic 618
- 559 alcohols and α -oxo ketene dithioacetals: synthesis of functionalized 619
- 560 cyclopentadienes and further application in a Diels–Alder reaction. 620
- 561 *Angew. Chem. Int. Ed.* **53**, 7209–7213 (2014) 621
- 562 28. Dudnik, A.S., Sromek, A.W., Rubina, M., Kim, J.T., Kel'in, A.V., 622
- 563 Gevorgyan, V.: Metal-catalyzed 1,2-shift of diverse migrating groups in 623
- 564 allenyl systems as a new paradigm toward densely functionalized hetero- 624
- 565 cycles. *J. Am. Chem. Soc.* **130**, 1440–1452 (2008) 625
- 566 29. Peng, L., Zhang, X., Zhang, S., Wang, J.: Au-catalyzed reaction of 626
- 567 propargylic sulfides and dithioacetals. *J. Org. Chem.* **72**, 1192–1197 627
- 568 (2007) 628
- 569 30. Johnston, B.D., Pinto, B.M.: Synthesis of thio-linked disaccharides by 629
- 570 1→2 intramolecular thioglycosyl migration: Oxocarbenium *versus* 630
- 571 episulfonium ion intermediates. *J. Org. Chem.* **65**, 4607–4617 (2000) 631
- 572 31. Yu, B., Yang, Z.: Stereoselective synthesis of 2-S-phenyl-2-deoxy- β - 632
- 573 glycosides using phenyl 2,3-*O*-thionocarbonyl-1-thioglycoside donors 633
- 574 *via* 1,2-migration and concurrent glycosidation. *Org. Lett.* **3**, 377–379 634
- 575 (2001) 635
- 576 32. Peng, L., Zhang, X., Ma, M., Wang, J.: Transition-metal-catalyzed rear- 636
- 577 rangement of allenyl sulfides: a route to furan derivatives. *Angew. Chem.* 637
- 578 *Int. Ed.* **119**, 1937–1940 (2007) 638
- 579 33. Eckstein, F., Gish, G.: Phosphorothioates in molecular biology. *Trends* 639
- 580 *Biochem. Sci.* **14**, 97–100 (1989) 640
- 581 34. Frey, P.A., Sammons, R.D.: Bond order and charge localization in 641
- 582 nucleoside phosphorothioates. *Science.* **228**, 541–545 (1985) 642
- 583 35. Barr, J.D., Bell, A.J., Ferrante, F., La Manna, G., Mundy, J.L., Timperley, 643
- 584 C.M., Waters, M.J., Watts, P.: Fragmentations and reactions of some 644
- 585 isotopically labelled dimethyl methyl phosphono and trimethyl 645
- 586 phosphoro thiolates and thionates studied by electrospray ionisation ion 646
- 587 trap mass spectrometry. *Int. J. Mass Spectrom.* **244**, 29–40 (2005) 647
- 588 36. Kuivalainen, T., Kostiaainen, R., Björk, H., Uggla, R., Sundberg, M.R.: 648
- 589 Fragmentation of protonated *O,O*-dimethyl *O*-aryl phosphorothionates in 649
- 590 tandem mass spectral analysis. *J. Am. Soc. Mass Spectrom.* **6**, 488–497 650
- 591 (1995) 651
- 592 37. Cooks, R.G., Gerrard, A.F.: Electron impact-induced rearrangements in 652
- 593 compounds having the P=S bond. *J. Chem. Soc. B.* 1327–1333 (1968) 653
- 594 38. Santoro, E.: The fragmentation of some alkyl thio-phosphate esters by 654
- 595 electron-impact. *Org. Mass Spectrom.* **7**, 589–599 (1973) 655
- 596 39. Zeller, L.C., Farrell, J.T., Kenttämaa, H.I., Kuivalainen, T.: Multiple- 656
- 597 stage mass spectrometry in structural characterization of organophospho- 657
- 598 rus compounds. *J. Am. Soc. Mass Spectrom.* **4**, 125–134 (1993) 658
- 599 40. Deng, M., Yu, T., Luo, H., Zhu, T., Huang, X., Luo, L.: Direct detection 659
- 600 of multiple pesticides in honey by neutral desorption-extractive 601
- 602 electrospray ionization mass spectrometry. *Int. J. Mass Spectrom.* **422**, 603
- 603 111–118 (2017) 604
- 604 41. Picó, Y., Farré, M., Soler, C., Barceló, D.: Confirmation of fenthion 605
- 605 metabolites in oranges by IT-MS and QqTOF-MS. *Anal. Chem.* **79**, 606
- 606 9350–9363 (2007) 607
- 607 42. Frisch, M., Trucks, G.W., Schlegel, H.B., Scuseria, G.E., Robb, M.A., 608
- 608 Cheeseman, J.R., Zakrzewski, V.G., Montgomery Jr., J.A., Stratmann, 609
- 609 R.E., Burant, J.C., Dapprich, S., Millam, J.M., Daniels, A.D., Kudin, 610
- 610 K.N., Strain, M.C., Farkas, O., Tomasi, J., Barone, V., Cossi, M., Cammi, 611
- 611 R., Mennucci, B., Pomelli, C., Adamo, C., Clifford, S., Ochterski, J., 612
- 612 Petersson, G.A., Ayala, P.Y., Cui, Q., Morokuma, K., Malick, D.K., 613
- 613 Rabuck, A.D., Raghavachari, K., Foresman, J.B., Cioslowski, J., Ortiz, 614
- 614 J.V., Stefanov, B.B., Liu, G., Liashenko, A., Piskorz, P., Komaromi, I., 615
- 615 Gomperts, R., Martin, R.L., Fox, D.J., Keith, T., Al-Laham, M.A., Peng, 616
- 616 C.Y., Nanayakkara, A., Gonzalez, C., Challacombe, M., Gill, P.M.W., 617
- 617 Johnson, B., Chen, W., Wong, M.W., Andres, J.L., Gonzalez, C., Head- 618
- 618 Gordon, M.E., Replogle, S., Pople, J.A.: Gaussian 03, Revision B.03. 619
- 619 Gaussian, Inc., Wallingford (2004) 620
- 620 43. Bortolini, O., Guerrini, A., Lucchini, V., Modena, G., Pasquato, L.: The 620
- 621 phenylsulfonium cation: electronic structure and gas-phase reactivity. 621
- 622 *Tetrahedron Lett.* **40**, 6073–6076 (1999) 622
- 623 44. Smit, W.A., Krimer, M.Z., Vorob'eva, E.A.: Generation and chemical 623
- 624 reactions of episulfonium ions. *Tetrahedron Lett.* **16**, 2451–2454 (1975) 624
- 625 45. Matsumoto, K., Kozuki, Y., Ashikari, Y., Suga, S., Kashimura, S., 625
- 626 Yoshida, J.-I.: Electrophilic substitution reactions using an electro- 626
- 627 generated ArS(ArSSAr)⁺ cation pool as an ArS⁺ equivalent. *Tet- 627*
- 628 rahedron Lett. **53**, 1916–1919 (2012) 628
- 629 46. Verhaeghe, P., Dumêtre, A., Castera-Ducros, C., Hutter, S., Laget, M., 629
- 630 Fersing, C., Prieri, M., Yzombard, J., Sifredi, F., Rault, S., Rathelot, P., 630
- 631 Vanelle, P., Azas, N.: 4-Thiophenoxy-2-trichloromethylquinazolines dis- 631
- 632 play *in vitro* selective antiparasitic activity against the human malaria 632
- 633 parasite *Plasmodium falciparum*. *Bioorg. Med. Chem. Lett.* **21**, 6003– 633
- 634 6006 (2011) 634
- 635 47. Niddam, V., Camplo, M., Le Nguyen, D., Chermann, J.-C., Kraus, J.-L.: 635
- 636 Thiophenoxy peptides: a new class of HIV replication inhibitors. *Bioorg.* 636
- 637 *Med. Chem. Lett.* **6**, 609–614 (1996) 637
- 638 48. Medou, M., Priem, G., Rocheblave, L., Pepe, G., Meyer, M., Chermann, 638
- 639 J.-C., Kraus, J.-L.: Synthesis and anti-HIV activity of α -thiophenoxy- 639
- 640 hydroxyethylamide derivatives. *Eur. J. Med. Chem.* **34**, 625–638 (1999) 640
- 641 49. Jiang, K., Bian, G., Hu, N., Pan, Y., Lai, G.: Coordinated dissociative 641
- 642 proton transfers of external proton and thiocarbamide hydrogen: MS 642
- 643 experimental and theoretical studies on the fragmentation of protonated 643
- 644 *S*-methyl benzenylmethylenhydrazine dithiocarboxylate in gas phase. 644
- 645 *Int. J. Mass Spectrom.* **291**, 17–23 (2010) 645
- 646 50. Kuck, D., Bather, W.: Inter- and intra-annular proton exchange in gaseous 646
- 647 benzylbenzenium ions (protonated diphenylmethane). *Org. Mass* 647
- 648 *Spectrom.* **21**, 451–457 (1986) 648
- 649 51. Newman, M.S., Kames, H.A.: The conversion of phenols to thiophenols 649
- 650 *via* dialkylthiocarbamates. *J. Org. Chem.* **31**, 3980–3984 (1966) 650
- 651 52. Prabhakar, S., Kar, P., Mirza, S.P., Lakshmi, V.V.S., Nagaiah, K., 651
- 652 Vairamani, M.: Mass spectral study of *O*- and *S*-aryl 652
- 653 dimethylthiocarbamates under electron impact conditions: Newman- 653
- 654 Kwart rearrangement in the gas phase. *Rapid Commun. Mass Spectrom.* 654
- 655 **15**, 2127–2134 (2001) 655